Optimal Design for CLIP EPDM Rubber Products using a Flow Analysis

Young-Min Huh[1], Kwang-O Lee[1,#] and Sung-Soo Kang[2]

1 Precision Mechanical Engineering, Pusan National University, Busan, South Korea
2 School of Mechanical Engineering, Pusan National University, Busan, South Korea
Corresponding Author: E-mail: royallko@pusan.ac.kr; Tel: +82-51-510-1454; Fax: +82-51-512-9635

KEYWORDS : Ethylene propylene diene monomer (EPDM), Optimal design, Gate location, Filling rate, CAE, Cross-WLF equation

Rubber is used in many industrial products, such as hoses, rubber belts, and oil seals. In particular, more than 200 rubber parts are used in automobiles. The design technology of these parts is largely dependent on field experience, which leads to lengthy and expensive developing procedures. However, with the help of recent developments in nonlinear computer analysis, new rubber products can be developed at low cost. In this study, rubber injection molding design variables, such as location and number of gates, were optimized using computer-aided engineering with the cross-WLF equation to produce CLIP rubber products made from ethylene propylene diene monomer (EPDM). The validity of the proposed design was evaluated by comparison with actual forming results.

Manuscript received: January 26, 2006 / Accepted: February 3, 2006

1. Introduction

Rubber is widely found in daily life, often used in machinery, automobiles, vibration control products, and oil seals and covers. One type of rubber, ethylene propylene diene monomer (EPDM), has a wide range of properties when mixed with carbon black additive, and is commonly used for rubber auto parts. Because of the complicated flow behavior of rubber, the design of rubber parts in the past was dependent on trial and error techniques and experience, which increased the development time and cost. But due to the rapid expansion of computer simulation technologies, many studies have now applied nonlinear flow analyses to organic materials such as rubber and plastics.[1-8] The results obtained from these studies have led to simultaneous cost reductions and quality improvements during the development of new products.

In this study, we conducted flow simulations of the injection process for manufacturing CLIP products, which are used to prevent interference in hydraulic pipes. By considering several design variables, such as location and number of gates, the simulated flow and filling behavior of the resin suggested an optimal design that will produce sound products. The proposed design conditions were then evaluated by the comparing the analyses with actual injection products.

2. Behavior of the EPDM material

2.1 Rheometer tests

Rheometer tests were conducted based on KS M 6518 standards to measure the desired vulcanization time of KEP-570F EDPM material, which was manufactured by Kumho Polymer Co. The temperature of both the upper and lower plates was 180°C in the tests. The torque loaded on the specimens was measured while the upper plate was fixed and the lower plate was rotated by 1 degree. This was then related to the index of vulcanization.

Fig. 1 shows the vulcanization time–torque relationship obtained in the rheometer tests. The vulcanization time was defined as 300 seconds from the start of a test until 90% of the vulcanization had occurred.

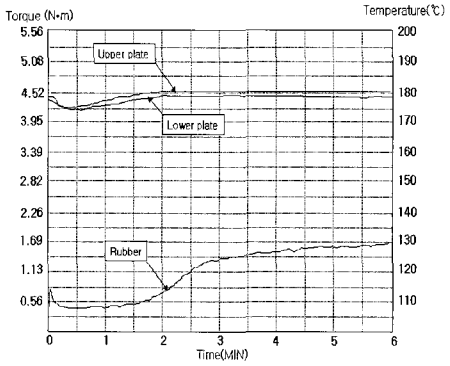

Fig. 1 Torque–time curves from the rheometer tests

2.2 Cross-WLF viscosity model

Viscosity is an important flow characteristic that represents the internal resistance to deformation of the material. It is described by the ratio of the shear stress (τ) and shear velocity:

$$\eta \equiv \frac{\tau}{\dot{\gamma}} \tag{1}$$

If the relationship of the above equation is linear, *i.e.*, the viscosity is independent of the shear velocity, the behavior of material is

Newtonian; otherwise, the behavior of the material is non-Newtonian. Rubber has Newtonian flow characteristics, and thus the Cross-WLF Model[11,12] is generally applied to represent its behavior:

$$\eta = \frac{\eta_0(T)}{1+\left(\frac{\eta_0(T)\dot{\gamma}}{\tau^*}\right)^{(1-n)}}$$

where η, T, n, and $\dot{\gamma}$ denote the viscosity, temperature, shear velocity sensitivity, and shear velocity, respectively, and τ^* is the shear stress at transition from Newtonian to non-Newtonian flow. Here, η_0 is the viscosity as the shear velocity gradually approaches zero,

$$\eta_0 = \lim_{\dot{\gamma}\to 0+} \eta = D_1 \exp\left[-\frac{A_1(T-T_g)}{A_2+(T-T_g)}\right]$$

where T_g is the glass transition temperature, and A_1, A_2, and D_1 are constants. The constants used in this study are listed in Table 1.

Table 1 Cross-WLF Model constants

Constant	Units	Value
η	–	0.3482
τ^*	Pa	17,900
D_1	Pa · s	1.12×10^8
A_1	–	8.0973
A_2	K	51.6
T_g	K	263.15

3. Flow analysis

3.1 One-gate system

Initially, a pre-simulation was performed to determine the best gate location. The results are shown in Fig. 2. The values in the figure indicate the preference index, which was scaled so that the value at the optimal location was 1.0. The preference index at each location was divided into three grades and denoted as ○, □, and X. The gate location for the one-gate system shown in Fig. 2 was selected based on the preference index and the thickness of the part. The flow injection system, consisting of the sprue, runner, and gate, was constructed at this location (see Fig. 3).

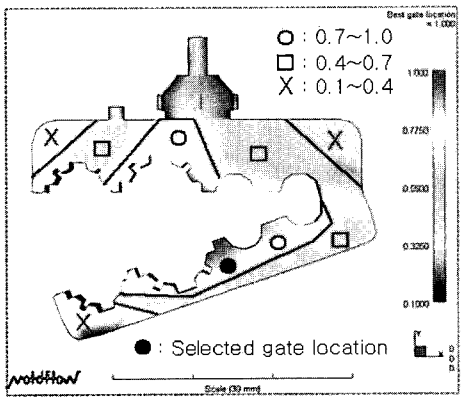

Fig. 2 Simulated preference index for the one-gate system

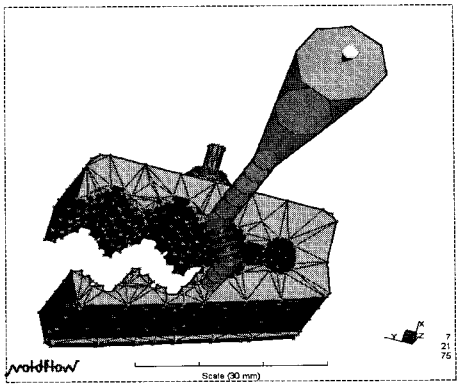

Fig. 3 Injection delivery system for the one-gate system

The pressure at an injector used in an actual forming process will gradually decrease when the amount of pumping is reduced by a factor of 3. Therefore, the pressure change with time at the injection point was considered in the simulations, as shown in Fig. 4. The figure indicates that 2.78 seconds were required to reach the maximum injection pressure of 16.6 MPa.

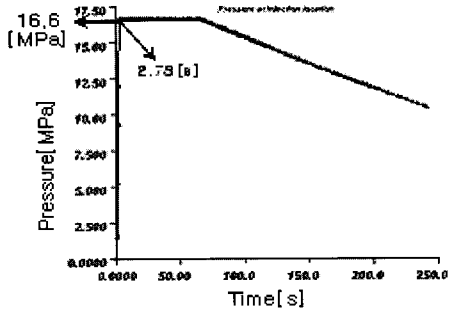

Fig. 4 Pressure change with time at the injection point of the one-gate system

Fig. 5 shows the filling results for the one-gate system. Under-filling occurred in both the A and B regions since the distance from the gate was large and the flow had to pass through the thin S area.

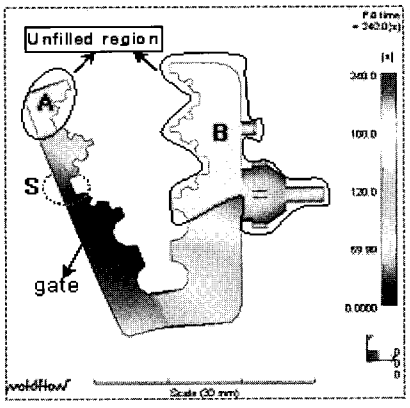

Fig. 5 Amount of filling in the one-gate system (under-filling occurred)

The mean velocity distribution at the end of the flow in the broad Q region was faster than that in the narrow P region, as shown in Fig. 6. Therefore, the quantity of flow that traveled to the P region was less than to the Q region.

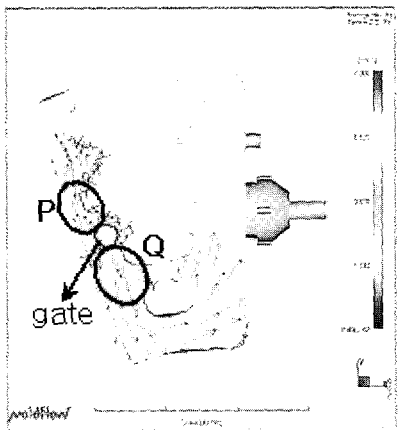

Fig. 6 Average velocity distribution at the end of the flows in the one-gate system

This is also apparent from the filling time, which is illustrated in Fig. 7. As the filling progressed, the flux to the X region did not generate any additional filling; the flow only traveled to the Y region. Additional gates are required in the Y region to promote flow to the X region and provide an increased volume in the Y region.

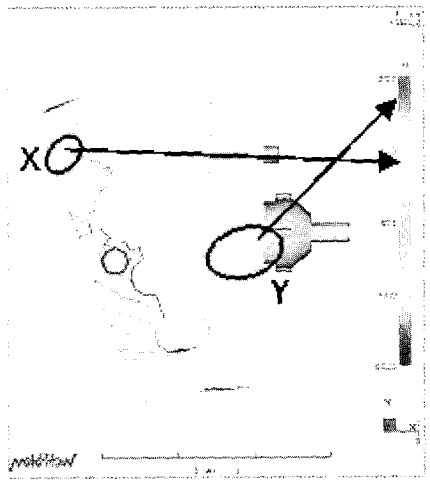

Fig. 7 Filling time at every location after the injection was completed

3.2 Three-gate system

A three-gate system was constructed, as shown in Fig. 8, based on the gate location flow analysis results of the one-gate system.

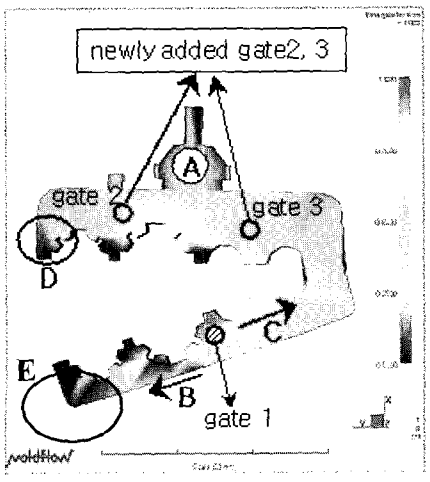

Fig. 8 Three-gate system and locations of the additional two gates

Gate 3 was added to protect the flow in the C direction as well as to induce flow into the Ⓐ region, in which a large volume was required. Gate 2 was added to fill the D region as well as to induce flow into the Ⓐ region. Like the one-gate system, the three-gate system was designed by considering the pressure change at the injection point with time. Except for the unfilled M region, there was an almost constant velocity distribution in every region, as indicated by the mean velocity at the end of each flow shown in Fig. 9. One additional gate was required to perfectly fill the unfilled region shown in Fig. 10.

3.3 Four-gate system

A new gate was added in the unfilled region based on the simulation results of the previous sections. The amount of pumping was increased by a factor of three to prevent a pressure drop during the injection. The resulting pressure change with time at the injection

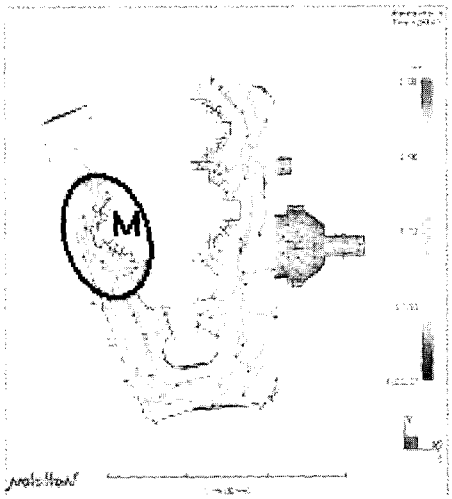

Fig. 9 Average velocity distribution at the end of the flows in the three-gate system

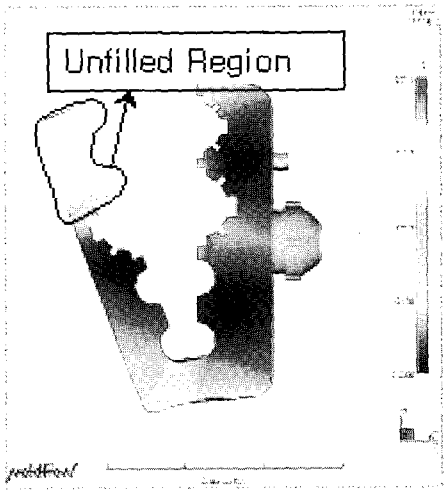

Fig. 10 Amount of filling in the three-gate system (under-filling occurred)

point was modeled in the simulation, similar to the one- and three-gate systems. Complete filling occurred after 284 seconds (see Fig. 11), which corresponded with the expected vulcanization time (about 300 s) from the rheometer test results.

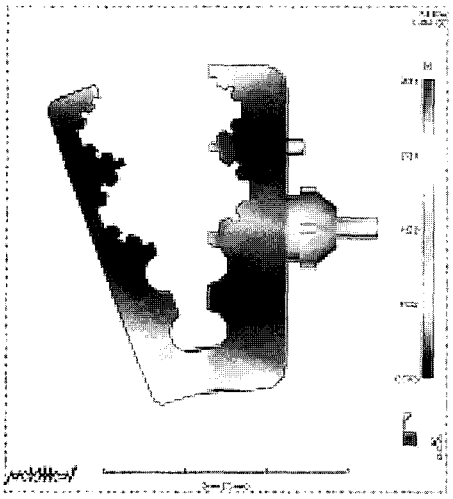

Fig. 11 Complete filling in the four-gate system

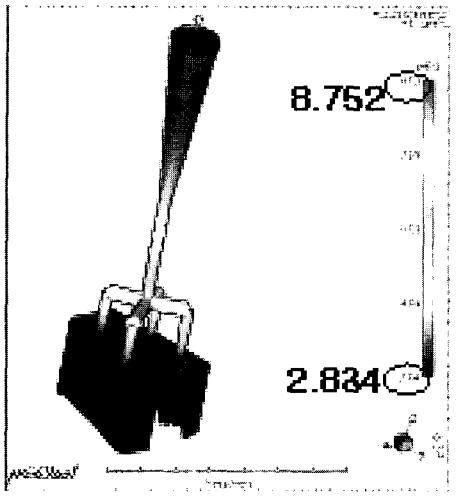

Fig. 12 Pressure distribution in the four-gate system after complete filling

Fig. 12 shows the pressure distribution and average velocity when complete filling occurred. The maximum pressure at the injection point decreased by about 50%, from 16.600 to 8,752 MPa. The minimum pressure after injection was 2.834 MPa, and the distribution of the mean flow velocity was uniform throughout the product (see Fig. 13).

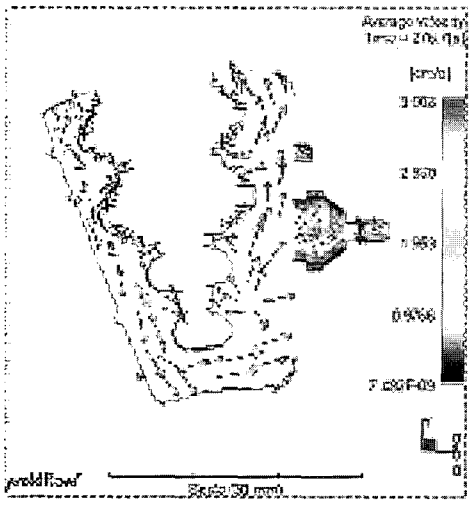

Fig. 13 Average velocity in the four-gate system after complete filling

4. Actual injection of CLIP products

Actual injection tests were performed using the one-, three-, and four-gate systems with the same conditions that were used for the numerical analyses. Fig. 14(a), (b), and (c) show the actual injection moldings of the one-, three-, and four-gate systems, respectively. In the one-gate system, under-filling occurred in the α region because of the pressure drop at the leading edge of the flow, and in the β region where the leading edge could not go pass through the thin region. These results are in accordance with the simulation shown in Fig. 5. In the three-gate system, the α region was completely filled due to the additional gates, but under-filling still occurred in region β. These results are also in agreement with the previous analysis shown in Fig. 10. In the four-gate system, a fourth gate was added to fill the α region. In the actual injection molding tests, 0.025–0.038-mm air vents were also installed at the air traps in the injection model, as shown in Fig. 15, because air confined in a cavity may create a defective product.

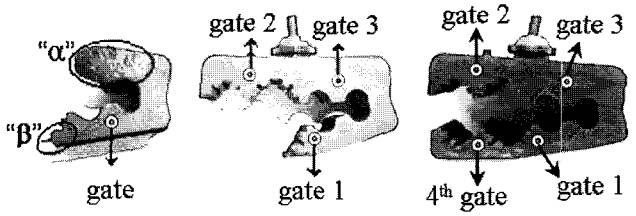

(a) one-gate system (b) three-gate system (c) four-gate system

Fig. 14 Actual injection products

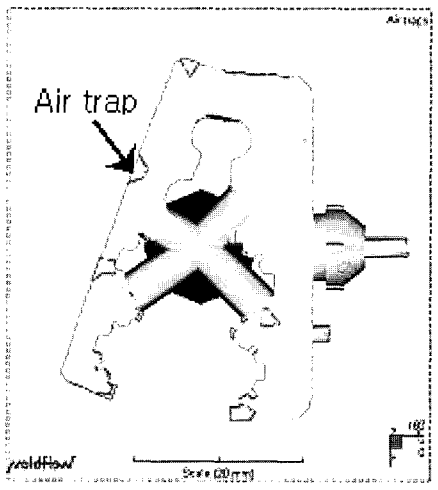

Fig. 15 Air trap distribution of the four-gate system

5. Conclusions

Flow simulations of the injection process used for CLIP products, which are made from EPDM rubber material, were conducted using a commercial code. The results were compared with actual injection products. The following conclusions were drawn.

1) The best gate location was determined using a pre-simulation, and the resulting flows predicted for an injection system with one gate, three gates, and four gates were analyzed. Under-filling occurred with the one- and three-gate systems, but a sound product was obtained with the four-gate system.
2) The factors that affected under-filling were the pressure drop at the leading edge, the presence of an air trap, and the pressure drop at the injection point.
3) The simulation results were in good agreement with actual

injection tests. The slight discrepancy that occurred in the amount of under-filling was due to the selection of the coefficients for the cross-WLF equation, which governs the viscosity of the rubber material.

4) Properly located air vents as well as constant pressure at the injection points are required to produce completely filled and high quality products.

REFERENCES

1. Harry, D. H. and Parrot, R. G., "Numerical simulation of injection mold filling," Polymer Engineering and Science, Vol. 10, No. 4, pp. 209-214, 1970.
2. Gao, F., Patterson, W. I. and Kamal, M. R., "Cavity pressure dynamics and self-tuning control for filling and packing phases of thermoplastics injection molding," Polymer Engineering and Science, Vol. 36, No. 9, pp. 1272-1285, 1996.
3. Swan, P. L., Garcia-Rejon, A., Cielo, P. and Kamal, M. R., "Optical on-line measurement of the thickness distribution of blow molding parisons," Polymer Engineering and Science, Vol. 36, No. 7, pp. 985-992, 1996.
4. Sherbelis, G., Morikawa, J. and Kurihara, T., "Thermal diffusivity of thermosetting materials by temperature–wave analysis source," Thermochimica Acta, Vol. 299, No. 2, pp. 95-100, 1997.
5. Lee, Y. B. and Kwon, T. H., "Modeling and numerical simulation of residual stresses and birefringence in injection molded center-gated disks," Journal of Materials Processing Technology, Vol. 111, No. 1/3, No. 25, pp. 214-218, 2001.
6. Hieber, C. A. and Shen, S. F., "A finite-element/finite-difference simulation of the injection-molding filling process," Journal of Non-Newtonian Fluid Mechanics, Vol. 7, No. 1, pp. 1-32, 1980.
7. Zu, Y. S. and Lin, S. T., "Optimizing the mechanical properties of injection molded W-4.9%Ni-2.1%Fe in debinding," Journal of Materials Processing Technology, Vol. 71, No. 2, pp. 337-342, 1997.
8. Ballman, R. L., Shusman, T. and Toor, H. L., "Injection molding flow of a molten polymer into a cold cavity," Industrial and Engineering chemistry, Vol. 51, pp. 847-850, 1959.
9. Ghosh, P. and Chakrabarti, A., "Effect of incorporation of conducting carbon black as filler on melt rheology and relaxation behaviour of ethylene–propylene–diene monomer (EPDM)," European Polymer Journal, Vol. 36, pp. 607-617, 2000.
10. Ginic-Markovic, M., Dutta, N. T., Dimopoulos, M., Choudhury, N. and Matisons, J. G., "Viscoelastic behaviour of filled and unfilled, EPDM elastomer," Thermochimica Acta, Vol. 357, pp. 211-216, 2000.
11. Sopade, P. A., Halley, P., Bhandari, B., D'Arcy, B., Doebler, C. and Caffin, N., "Application of the Williams–Landel–Ferry model to the viscosity temperature relationship of Australian honeys," Journal of Food Engineering, In Press, Uncorrected proof available online 14 May 2002.
12. Ferry, J. D., "Viscoelastic Properties of Polymer," John Wiley & Sons, New York, pp. 280-290, 1980.